Notes

Quantitative Characterization of Librational Rate Distributions for G2 PAMAM Dendrimer Salt from Deuteron Magic Angle Spinning Spectra

Dariya I. Malyarenko,† Robert L. Vold,*,† and Gina L. Hoatson‡

Departments of Applied Science and Physics, The College of William and Mary, P.O. Box 8795, Williamsburg, Virginia 23187-8795

Received March 29, 2001

Introduction

Polyamidoammonium (PAMAM) chloride dendrimer salts are hyperbranched polymers synthesized from an ethylenediamine core and terminated with ammonium groups. The spacers, containing amide groups, are formed by addition of ethylenediamine and sodium acrylate molecules. They connect protonated tertiary amine branching points in PAMAM salts. For instance, generation 2 (G2) dendrimer has 16 terminal RND_3^+, 28 spacer R_2ND, and 14 branching R_3ND^+ groups. Like other dendrimer generations, G2 exhibits a very broad glass transition (294−344 K). This behavior has recently been analyzed for six PAMAM generations using deuteron quadrupole echo (QE) line shapes[1] and spin relaxation time (T_{1Z}) anisotropies.[2] NMR spectra of all dendrimer generations consisted of three overlapping powder patterns originating from three chemically distinct deuterated sites in rigid glassy dendrimers. Their temperature dependence provided quantitative characterization of librational motion of the dendrimer spacer and branching point and revealed a composite, two-frame motion of ammonium termini. However, the QE and T_{1Z} experiments showed little sensitivity to librational motion of the dendrimer termini. This note presents deuteron magic angle spinning (^{2}H MAS) results for generation 2 PAMAM ammonium-d_3 chloride salt. It will be shown that the ^{2}H MAS line shapes provide quantitative information about libration of the dendrimer termini. In addition, they permit characterization of distributions of libration rates at the dendrimer spacers. These are surprisingly narrow for PAMAM salts. Implications of these results for theories of dendrimer formation and structure are discussed.

Experimental Methods

Sample preparation and handling procedures are described in refs 1 and 2. All experimental spectra were collected on a home-built spectrometer, operating at 46.06 MHz, using a Chemagnetics MAS triple resonance probe with a 5 mm coil, tuned in single channel mode. The quality factor of the probe is $Q = 220$, determined by matching a line shape simulation to a QE experiment on deuterated polyethylene. 90° (3 μs) pulses were applied with 1 s recycle delay in single pulse experiment with a 100 kHz spectral width. Magic angle spinning rate was 4000 ± 2 Hz. The sample was packed under a nitrogen atmosphere into a rotor sealed with two finned spacers to protect it from moisture. Thermal equilibration was allowed to proceed for 20 min before data acquisition. The number of scans was limited by heat conduction to the magnet (typically, less than an hour including thermal equilibration at the extreme temperatures).

Simulations were performed by numerically solving the stochastic Liouville−von Neumann equation for a statistical ensemble of deuterons subject to discrete random reorientational process under MAS conditions,[3] according to specified motional models.[1] For the spacer (R_2ND) and branching site (R_3ND^+) deuterons we used the model of random jumps between six sites on a planar arc of amplitude ϕ, at rate k_1. The arc is in the plane containing the q_{xx} and q_{zz} components of deuteron electric field gradient tensor. For terminal (RND_3^+) deuterons, single frame libration in a cone, β_c, was modeled by jumps among four sites as described in ref 2. These models provided adequate description of both temperature-dependent QE line shapes and T_{1Z} anisotropies in our previous studies.[1,2] A large population, p_4, was used for the single orientation described by Euler coordinates Ω_4(240°, β_c, 0°), and equal populations were assigned to the other three sites, $p_{1,2,3} = (1 - p_4)/3$. Quadrupole coupling parameters, averaged by a fast 3-fold rotational motion ($k_3 > 10^9$ s^{-1}), were fixed to the values $\eta = 0$ and $\chi = 55$ kHz. The inclusion of an additional frame with an explicit 3-fold motion was not necessary due to the fast rate of this motion[2] and would only lengthen the simulation time. The calculation of each MAS spectrum took 100−120 min of CPU time on an SGI O2 workstation.

Because of hardware limitations (narrow probe bandwidth, relatively long pulses, and imperfect thermal isolation), we did not expect to get adequate spectral coverage for full characterization of the broad spectra from R_2ND and R_3ND^+ deuterons ($\chi \sim 150$−200 kHz). Their wide powder patterns, broken into spinning sidebands, underlay the narrowest, contributed by RND_3^+ deuterons.

Results

After proper correction for the finite pulse width and the probe *Q*-factor, the simulation of underlying powder patterns from spacer and branching point deuterons (Figure 1b) shows an almost flat intensity pattern across the frequency range of the motionally averaged spectrum of ammonium termini. Therefore, these contributions do not influence the intensity pattern in the middle of the spectra, which we are to analyze in terms of RND_3^+ dynamics. We also conclude that at any temperature the contribution from the spacers will not exceed the values observed between 50 and 70 kHz. This allows us to neglect completely spacer contributions for temperatures above 290 K (see inset c in Figure 1).

Spinning sidebands for the secondary amide and the tertiary amine deuterons (Figure 1c) become slightly narrower with decreasing temperature, which can be accounted for in simulations either by slightly increas-

† Department of Applied Science.
‡ Department of Physics.
* To whom correspondence should be addressed. e-mail: rlv@nmr.physics.wm.edu.

10.1021/ma0105385 CCC: $20.00
Published on Web 09/27/2001

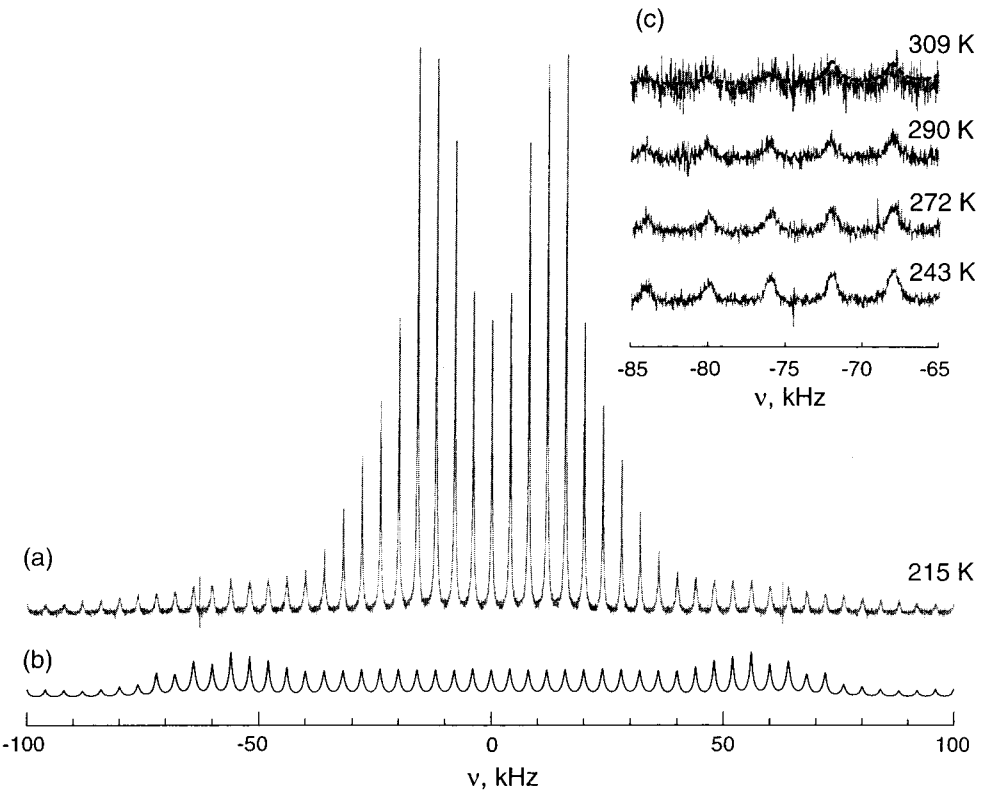

Figure 1. Experimental ^{2}H MAS spectrum (a) for PAMAM G2 at 215 K is compared with a one-frame arc libration simulation (b) for R_3ND^+, $k_l = 4.0 \times 10^5$ s^{-1}, $\phi = 11°$, and R_2ND, $k_l = 1.0 \times 10^6$ s^{-1}, $\phi = 19°$. The motion is modeled by jumps between six sites of equal populations on an arc of amplitude ϕ, with quadrupole coupling parameters: $\chi_{PAS} = 162$ kHz, $\eta_{PAS} = 0.05$, and $\chi_{PAS} = 209$ kHz, $\eta_{PAS} = 0.12$, for above-mentioned deuteron sites, respectively. The inset (c) illustrates the broadening and decreasing S/N for the outer parts of the experimental spectra with the increasing temperature. The bold line through the spectrum at 309 K shows the fit for R_2ND component only, with $k_l = 0.9 \times 10^6$ s^{-1} and $\phi = 19°$.

ing the rate of libration or by decreasing the arc angle. The latter makes more physical sense. Trying to find librational rates to fit the sideband line width at $T <$ 290 K, we notice that extrapolation of librational rates to lower temperatures from Arrhenius fits obtained previously from temperature-dependent spin−lattice relaxation measurements for $T >$ 295 K[2] is definitely not possible. If done ($k \sim 10^3$−10^4 s^{-1}), this would give very broad lines even for angles as small as 1°−5°, which is not observed experimentally. Instead, librational rates, k_l, on the order of 10^5−10^6 s^{-1} for both R_2-ND and R_3ND^+ deuterons provide adequate fits for $T <$ 290 K. At these temperatures the values show almost no temperature dependence, which is expected behavior for librational motion.[4] Therefore, we conclude that the unusually high activation energies, reported previously[2] for libration at higher temperatures, must be connected with the onset of the glass transition around $T =$ 294 K[1] accompanied by hydrogen bond disruption.[2] Any extrapolation from the corresponding Arrhenius fits must be confined to the glass transition region for the dendrimers.

In addition, the low temperature data allow us to address the question of motional rate distributions, putting limits on their width. Description of relaxation and motional processes in polymers are often based on the log-normal rate distribution[5] or empirical variations.[6] These distributions are normal on the "log" scale and are therefore skewed, with long tails toward higher rates, on the linear rate scale. The simplest form found to be adequate for description of the present data is

$$G(k_i) = N^{-1} \exp\left(-\frac{1}{2}\left(\frac{\log(k_i) - \log(k_{mp})}{\sigma_k}\right)^2\right) \quad (1a)$$

where

$$N = \sum_{i=0}^{n_k-1} \exp\left(-\frac{1}{2}\left(\frac{\log(k_i) - \log(k_{mp})}{\sigma_k}\right)^2\right) \quad (1b)$$

For each rate, k_i, the simulated spectrum was normalized to unit total intensity before multiplying by the corresponding weight $G(k_i)$. Then the total spectrum is calculated as a sum of n_k subspectra for k_i values sampled from the distribution, $I(\nu) = \sum_{i=0}^{n_k-1} I(\nu,k_i)G(k_i)$. It was usually sufficient to use three to five rates with $k_i = k_{mp} \times 10^{\pm i\sigma_k}$, $i = \overline{0,(n_k-1)/2}$, chosen symmetrically around the most probable value k_{mp} for an adequate sampling of the distribution, with $\sigma_k < 1$. In this case corresponding weights reduce to

$$G(k_i) = \frac{\exp\left(-\frac{i^2}{2}\right)}{1 + 2\sum_{i=1}^{(n_k-1)/2} \exp\left(-\frac{i^2}{2}\right)} \quad (2)$$

We emphasize here that the most probable rate, k_{mp}, is always less than the average rate, $\bar{k} = \sum k_i G(k_i)$, due to the logarithmic form of the distribution. The fraction of spins with rates faster than k_{mp} is larger than that with the rate slower than k_{mp} and will contribute more

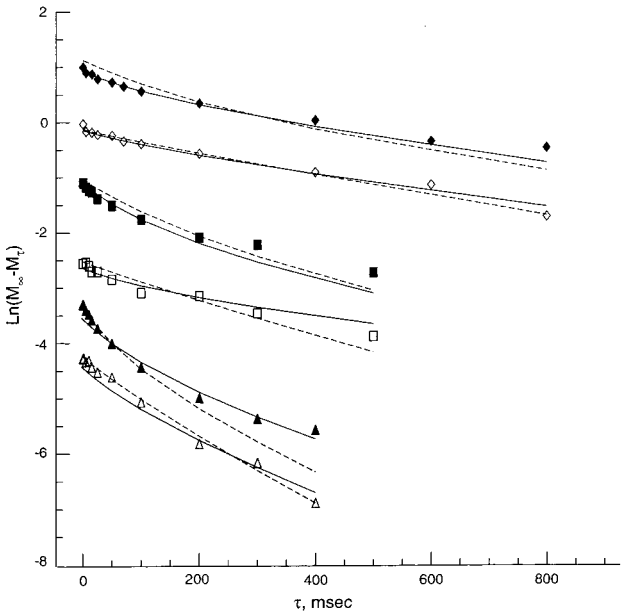

Figure 2. Experimental (symbols) and EXPRESS simulated (lines) T_{1Z} recovery curves for G2 at 298 K (diamonds), 308 K (squares), and 318 K (triangles). Filled symbols correspond to slices on the line shape at 50 kHz and open symbols to 80 kHz. Two different fits are shown, $\sigma_k = 0.0$ (dashed lines); $\sigma_k = 0.5$ (solid lines) for both underlying powder patterns at 298 and 308 K, and $\sigma_k = 0.4$ and 0.6 for spacers and branching points, respectively, at 318 K. The fit parameters and models are the same as in ref 2, except for the most probable librational rate in rate distribution simulation for R_3ND^+ at 318 K, $k_{mp} = 1.2 \times 10^7$ s^{-1}. The data are vertically shifted for clarity.

intensity to the spectrum. Thus, the prevailing contribution to the spectral intensity will come from spins moving with the rates closer to $\bar{k}$.

The distribution of rates can have major effects on the line width of the MAS sidebands, even when the overall intensity envelope is not greatly affected. The sideband intensity envelope (powder pattern) depends predominantly on the librational amplitude and site populations. For the low temperature data, we found that no distribution is necessary. In fact, any distribution with $\sigma_k > 0.4$ would yield both very narrow and very wide components for the lines, and this is not observed experimentally. For the high temperature data, the S/N is insufficient for a quantitative analysis. However, attempts to fit the spectrum at 309 K with the same rates as derived from inversion recovery T_{1Z} anisotropy measurements[2] show that the model is sufficient for R_2ND deuterons (Figure 1).

Some reconsideration of the R_3ND^+ librational rates is needed. For this motion, the T_{1Z} data[2] give $k_l \sim 10^7$; however, this should produce very narrow sidebands which are not present in the MAS spectrum. Clarification can be achieved by revisiting the spin−lattice relaxation data.[2] Figure 2 shows experimental recovery curves for G2 at several temperatures increasing from top to bottom.

The dashed lines mark the results of simulations done with no rate distribution, using the EXPRESS algorithm.[7] The solid lines represent EXPRESS fits with five rates sampled from the log-normal distribution with $\sigma_k = 0.5$ and k_{mp} the same as k_l for the single rate fits at 298 and 308 K. At 318 K, $k_{mp} = 1.2 \times 10^7$ s^{-1}, and $\sigma_k = 0.4$ and 0.6 for spacers and branching points, respectively. We found only minor differences between the three-rate and five-rate fits in this rate range. The data marked by filled symbols correspond to intensities at 50 kHz from the center of the spectrum, where the prevailing contribution comes from the R_3ND^+ powder pattern. The open symbols mark the 80 kHz slice, where R_2ND deuterons contribute the most.

From Figure 2 (see caption) we see that there is little change in distribution width with increasing temperature (other then maybe more narrowing) at 80 kHz. For the 50 kHz recovery curves, the distribution width increases with temperature, and the fits assuming no distribution reproduce well only the first few data points ($\tau < 200$ ms) with higher average slope (shorter T_{1Z} values), corresponding to higher libration rates. For R_3ND^+, the k_{mp} used at higher temperatures is found to be lower than k_l used in previous EXPRESS simulations.[2] The latter were derived by matching intensity contributions for relaxation delays $\tau < 200$ ms (Figure 2) and in that sense should be close to the $\bar{k}$ of the skewed distribution. The slight decrease in k_{mp} with increasing temperature is consistent with the absence of narrow sidebands in the high temperature MAS spectra. The activation energies derived previously[2] for librational motion of the dendrimer spacers can now be identified with the average characteristic temperature dependence of $\bar{k}$. Of course, introduction of the librational rate distribution will increase uncertainty of the best fit rates and activation energies but does not alter the basic trends and conclusions reported previously.[2]

For the ammonium termini, interpretation of the MAS spectra (Figure 3) is complicated due to a possible distribution of librational angles, β_c, which can produce changes both in intensity envelope and in sideband line widths. However, it is natural to assume that a distribution of hydrogen bond length (as is the case for the branching site deuterons R_3ND^+)[1] is at least partially responsible for the observed 5 kHz line width of the RND_3^+ powder pattern in the quadrupole echo experiments. If the distribution of ammonium PAS quadrupole coupling constants has the same width as for tertiary amine deuterons at the branching points, $\sigma_\chi \sim 8$ kHz, averaging over the fast 3-fold rotation leaves less than 2 kHz width to be accounted for by β_c distribution. Thus, σ_β is at most 5°−6°. Such a narrow distribution of librational angles can be neglected for MAS spectra interpretation, since simulations show that σ_β larger than 15° is needed to noticeably affect the MAS line width or intensity patterns.

Our previous results[2] suggested that there are two overlapping powder patterns, coming from "fast" and "slow" ammonium rotors. This model can match the intensity pattern and width for low temperatures ($T <$ 290 K) but introduces double the number of fit parameters. Also, this does not apply to higher temperatures ($T >$ 309 K), where the fraction of "fast" ammonium rotors is less than 5%.[2] Searching for a single model, with the least number of fit parameters, to produce adequate fits for both the intensity pattern and the line width of all the temperature-dependent MAS data (Figure 3), we settled on the model of librational motion in an asymmetric cone. The asymmetry is modeled by a high population at one of the cone sites. This population difference is essential to reproduce the intensity pattern around the horns of the RND_3^+ powder pattern. Temperature dependent changes in the intensity pattern across the horns from concave downward to concave upward (see Figure 3), and also the change in the line widths, were accounted for by introduction of a log-

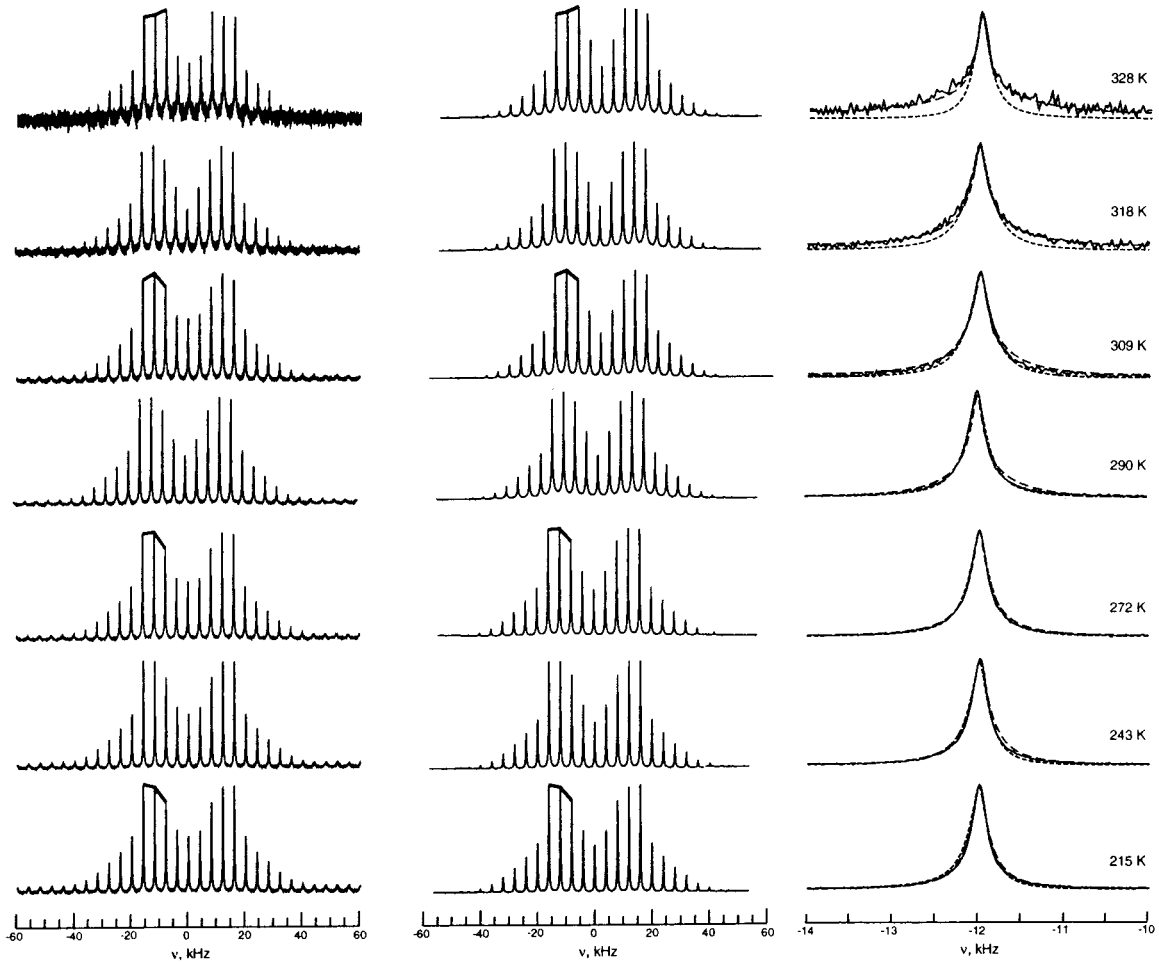

Figure 3. Experimental temperature-dependent ^{2}H MAS spectra (left column) and best fits (middle column) for RND_3^+ groups of G2 dendrimer. The right column compares experimentally observed line width for rotation sideband of the highest intensity with the simulations assuming zero (short dashes) and finite (long dashes) distribution width for cone libration rates, k_c. All corresponding fit parameters are listed in Table 1. The bold line over the left horn of every other experimental and simulated spectrum is shown to emphasize the change in intensity pattern with increasing temperature.

Table 1. Best Fit Parameters for Temperature Dependent ^{2}H MAS Spectra of G2 PAMAM Dendrimer

$T \pm 0.4$, K	$\beta_c \pm 1$, deg	$p_4 \pm 0.003$	$k_{mp} \times 10^6$, s^{-1}	$\sigma_k \pm 0.02$	$\overline{k_c} \times 10^6$, s^{-1}
214.9	33	0.880	1.5 ± 0.1	0.20	2.1 ± 0.5
242.7	33	0.871	1.4 ± 0.1	0.24	2.2 ± 0.5
271.6	34	0.874	1.3 ± 0.1	0.33	3.1 ± 0.8
289.9	35	0.877	1.2 ± 0.1	0.37	3.5 ± 0.9
308.9	36	0.871	0.90 ± 0.05	0.48	4.8 ± 0.9
318.1	36	0.862	0.70 ± 0.05	0.62	6.9 ± 1.1
327.6	45	0.892	0.43 ± 0.02	0.91	9.9 ± 0.7

normal distribution of the librational rates with fixed librational angle, β_c. Without this distribution, reasonably good fits may also be obtained for the low-temperature data with a fixed rate 1.6×10^6 s^{-1} and β_c changing from 30° to 40°. But for temperatures above $T = 309$ K, the line width cannot be fit properly (Figure 3, right column (short dashed lines)) using the single rate model. On the other hand, the three rates sampled from the log-normal distribution as described above ($k_0 = k_{mp}$, $k_{1,2} = k_{mp} \times 10^{\pm\sigma_k}$) were enough to obtain adequate fits for all temperature dependent MAS spectra (Figure 3 (long dashed lines)). The corresponding fit parameters are listed in Table 1.

The distribution width is small for the temperatures below 309 K and grows within the glass transition region of G2 (293 K < T < 343 K[1]). In fact, plotting the distribution width vs temperature (see Figure 4 (triangles), right scale) shows a sharp increase in the width of the distribution in the temperature region between 290 and 300 K. This is the region of the glass transition onset. Therefore, the considerable growth of the distribution width is correlated with the glass transition in the dendrimer. The most probable rates, k_{mp}, decrease for higher temperatures. But, as was emphasized above, it is the growing average rate, $\overline{k_c}$, that carries information about the prevailing spin contribution to the spectral intensity. The presence of a significant libration rate distributions is confined to the glass transition region of G2 dendrimer and does not influence the rates of 3-fold rotation determined from our previous spin relaxation data.[2]

The temperature dependence of the average librational rates, $\overline{k_c}$, for ammonium termini of G2 dendrimer is shown in Figure 4 (left scale). It is obvious that a single Arrhenius plot is impossible to construct for the full temperature range. However, two temperature regions can be approximately identified where the fits (indicated by dashed lines in Figure 4) are reasonably accurate. The first is for temperatures below 290 K and gives a very low activation energy $E_a = 3.8$ kJ/mol, which is physically reasonable for librational motion. The other, for temperatures within the glass

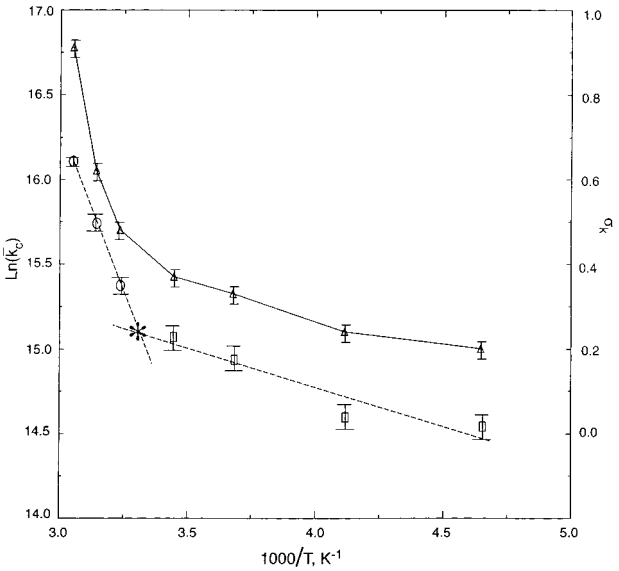

Figure 4. For G2 PAMAM dendrimer the plot presents the temperature dependence of the rate distribution width (triangles, right-hand scale) and average rates of termini libration (squares and circles), and Arrhenius fits (dashed lines, left-hand scale) for the temperatures below the glass transition onset (squares, $E_a = 3.8 \pm 0.9$ kJ/mol, $\ln(A) = 16.6 \pm 0.4$) and within the glass transition region (circles, $E_a = 32.8 \pm 0.1$ kJ/mol, $\ln(A) = 28.2 \pm 0.1$). The star marks a change in the slope at $T = 300 \pm 1$ K, which is close to the glass transition onset ($T = 294$ K). The $\bar{k}_c$ rates were calculated for the discrete distributions sampled from 6×10^3 to 3×10^7 s^{-1} with the step 5×10^3 s^{-1}. The solid line for σ_k (right scale) is drawn to guide an eye. The characteristic distribution parameters were derived from fitting experimental ^{2}H MAS spectra for G2. The quoted error limits for $\ln(\bar{k}_c)$ are obtained by error propagation from the uncertainties for k_{mp} and σ_k determined from the simulations.

transition region (to the left of "star"), shows a much higher slope with $E_a = 32.8$ kJ/mol.

Discussion

The meaning of the activation energy introduced here is different from that discussed in ref 5, where it is associated with k_{mp} rather than $\bar{k}_c$. We believe association of the observed activation energy with the average instead of the most probable rate carries more physical sense for highly skewed log-normal distributions. It is interesting that the approximate point of change in the slope ($T = 300$ K) is very close to the onset of the glass transition ($T = 294$ K) for G2 determined from DSC data.[1] Therefore, we argue that the observation of unusually high librational activation energies are intimately connected with the glass transition.

This is supported by MAS data for spacer deuterons discussed previously in this note. It seems reasonable to conclude that for R_2ND deuterons the distribution of rates (if any) stays narrow with the increasing temperature. So, the k_{mp} values stay close to $\bar{k}$ or at least have the same temperature dependence since the distribution skew does not change much with the temperature. On the other hand, the motional rate distribution width increases slightly for R_3ND^+ libration (up to $\sigma_k = 0.6-0.8$). The difference in behavior of librational rate distribution width with increasing temperature for deuterons at the branching points, R_3ND^+, and spacers, R_2ND, suggests that in the broad glass transition region the chlorine anions associated with deuterated branching points are partially responsible for increasing rate distribution width.

Finally, we stress that our results rule out any broad distribution of motional rates for solid dendrimer salts. Thus, solid PAMAM dendrimers behave very differently from linear glassy polymers[5] or dendrimers in solution, where at least three-decade distributions have been reported.[8,9]

Conclusions

In solid PAMAM dendrimers ^{2}H MAS line shapes provide quantitative information about librational motion, which is not accessible from either quadrupole echo[1] or Zeeman relaxation time[2] experiments. In particular, it is possible to characterize log-normal librational rate distributions at all major dendrimer sites: branching points, spacers, and termini. Taking into account the motional rate distributions also produces better fits for experimental Zeeman recovery curves. Introduction of a hydrogen bond length distribution causes the distribution of PAS quadrupole coupling parameters[1] but does not influence the line width of MAS spectra. Our ^{2}H MAS data support the validity of the motional models used for the analysis of temperature dependent quadrupole echo line shapes[1] and relaxation anisotropies.[2]

The onset of temperature activated librational motion and the sharp growth in librational rate distribution width coincide with the onset of the glass transition. This suggests that at temperatures below the glass transition onset dry dendrimers possess highly uniform intra- and intermolecular environments, in agreement with a kinetic dendrimer growth model.[10] The fact that in solid PAMAM dendrimers the distribution width is more strongly temperature dependent for the branching and terminal sites (with associated chlorine anion) demonstrates the sensitivity of dendrimer glass transition dynamics to the nature of counterion, solvent, or any foreign inclusion.

Acknowledgment. This work was supported by NSF Grants CHE 9701014 and DMR 9973933. Authors are grateful to Dr. J. H. Kristensen for providing the program for the rate dependent MAS spectra simulations.

References and Notes

(1) Malyarenko, D. I.; Vold, R. L.; Hoatson, G. L. *Macromolecules* **2000**, *33*, 1268−1279.
(2) Malyarenko, D. I.; Vold, R. L.; Hoatson, G. L. *Macromolecules* **2000**, *33*, 7508−7520.
(3) Kristensen, J. H.; Hoatson, G. L.; Vold, R. L. *Solid State NMR* **1998**, *13*, 1.
(4) Wittebort, R. J.; Olejniczak, E. T.; Griffin, R. G. *J. Chem. Phys.* **1987**, *86*, 5411−5420.
(5) Wehrle, M.; Hellmann, G. P.; Spiess, H. W. *Colloid Polym. Sci.* **1987**, *265*, 815−822.
(6) Connor, T. M. *Trans. Faraday Soc.* **1964**, *60*, 1574−1591.
(7) Vold, R. L.; Hoatson, G. L.; Tse, T. Y. *Chem. Phys. Lett.* **1996**, *263*, 271−273.
(8) Meltzer, A. D.; Tirrell, D. A.; Jones, A. A.; Inglefield, P. T. *Macromolecules* **1992**, *25*, 4549−4552.
(9) Meltzer, A. D.; Tirrell, D. A.; Jones, A. A.; Inglefield, P. T.; Hedstrand, D. M.; Tomalia, D. A. *Macromolecules* **1992**, *25*, 4541−4548.
(10) Lescanec, R. L.; Muthukumar, M. *Macromolecules* **1990**, *23*, 2280−2288.

MA0105385